EXTRACTION OF THE GLUON DENSITY FROM OPEN CHARM AT H1

D. MÜLLER

for the H1 Collaboration

Physik–Institut der Universität Zürich, Winterthurerstrasse 190, CH-8057 Zürich

E-mail: dmueller@physik.unizh.ch

In a large kinematical range of HERA, the production of open charm mesons is dominated by photon–gluon–fusion *(PGF)*. This allows to approximately calculate the momentum of the incoming gluon from the final state of the event. Using Next–to–Leading–Order *(NLO)* calculations, the gluon density has been extracted from measured cross sections of the process $ep \to eD^{\star\pm}X$ in both deep inelastic scattering and photoproduction.

1 Cross section measurements

In the two analyses presented here, charm production has been tagged through the decay chain $c \longrightarrow D^{\star+} \longrightarrow D^0\pi_s^+ \longrightarrow K^-\pi^+\pi_s^+$ (+ c.c.). Cuts on the transverse momenta ($p_\perp$) and polar angles of the particles in the final state guarantee a reliable measurement and suppress combinatorial background, but limit the range in $p_\perp$ and rapidity (pseudorapidity) of the $D^\star$, for which cross sections are given.

In the **deep inelastic scattering** *(DIS)* **analysis** [1], the kinematics of the scattering process have been measured using the hadronic final state as well as the scattered electron *(eΣ method* [2]*)*. This allows an accurate measurement over the full kinematic range and requires only small radiative corrections. The data have been corrected for detector effects and event losses through the imposed selection cuts by using a full simulation of the detector and the *AROMA* Monte Carlo generator, which describes the distribution of the data within statistical errors. In the kinematical range given in Table 1 , the cross section for $ep \to eD^{\star\pm}X$ has been measured to be $5.63 \pm 0.66(stat)^{+0.85}_{-0.68}(syst)$ nb (see also Figure 1).

In the **photoproduction (γp) analysis** [3], the photon energy (y) has been determined from the signals of the low angle electron taggers, located some 40 meters downstream the electron beam. Event losses due to their limited acceptance have been corrected by applying weights to the events. Differential cross sections are measured in different kinematic regimes as given in Figure 2 and Table 1 .

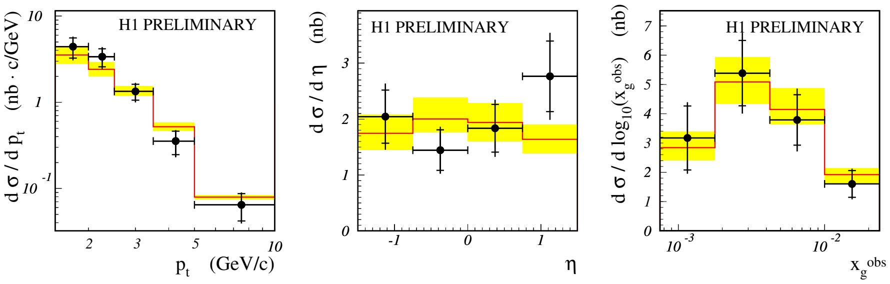

Figure 1: Cross sections for $ep \to eD^{\star\pm}X$ in DIS within the visible range given in Table 1, as a function of $p_\perp$ and pseudorapidity of the $D^\star$ and of $log(x_g^{obs})$. The data points are compared to the prediction of the NLO calculation [4] based on the GRV(HO) gluon density (histogram). The grey band indicates the uncertainty of the calculation due to the unknown charm quark mass.

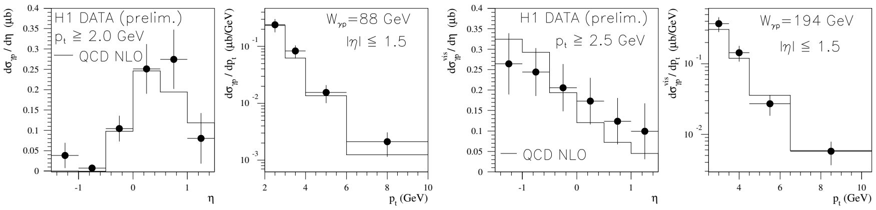

Figure 2: $d\sigma(\gamma p \to c\bar{c}X)/dp_\perp$ and $d\sigma(\gamma p \to c\bar{c}X)/d\eta$. The two plots on the left are measured at $W = 88$ GeV whereas the plots on the right correspond to the last two columns of Table 1. The data points are compared to the NLO calculation [5] (histogram).

2 Extraction of the gluon density

In a leading order picture, the momentum of the incoming gluon, which fuses with the photon, can be reconstructed from the measured photon and charm–quark kinematics [4]. Since we experimentally measure the $D^\star$ momentum, the following definitions, which show a good correlation to the actual gluon momentum, are used:

$$z = \frac{P \cdot p_{D^\star}}{P \cdot q} = \frac{(E-p_z)^{lab}_{D^\star}}{2E_e y} \qquad \hat{s} = \frac{(1.2 \cdot p_\perp^\star)^2 + m_c^2}{z(1-z)} \qquad x_g^{obs} = \frac{\hat{s}+Q^2}{ys} \tag{1}$$

Here P denotes proton four-vector, q the photon momentum and p the four momentum of the $D^\star$. $p_\perp^\star$ is measured in the γp system, with respect to the proton direction. In the range of the DIS analysis, x_g^{obs} is about an order of magnitude larger than x_{Bj}.

The measured cross section as a function of $log(x_g^{obs})$ can be compared

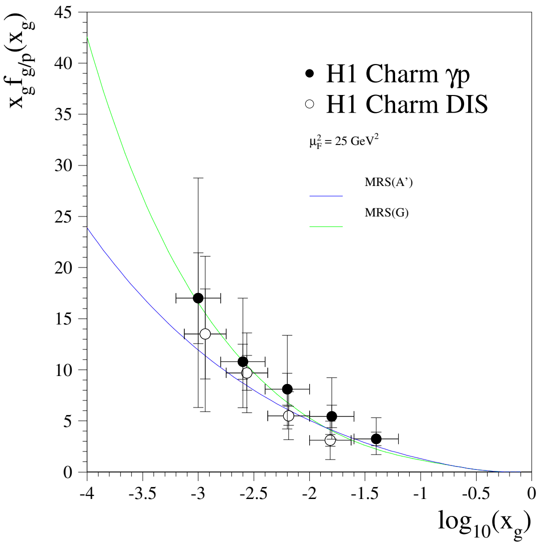

Figure 3: Comparison of the gluon densities obtained from the two $D^\star$ analyses. The systematic error of the DIS analysis is a quadratic sum of all contributions, dominated by the uncertainty of the charm quark mass and the fragmentation parameter. In the γp analysis, the systematic uncertainties from the theory are added linearly. The uncertainty is dominated by the scale dependence which includes the dependence on the charm quark mass.

to theoretical expectations which are given by the product of the gluon density $f_{g/p}(x)$ with the hard partonic cross section $\hat{\sigma}$ smeared by the correlation function $A(x_g^{true}, x_g^{obs})$, which absorbs the NLO contributions and the fragmentation effects.

$$\frac{d\sigma^{theo}_{ep\to eD^\star X}}{d\log\left(x_g^{obs}\right)} = BR_{(c\to D^\star)} \cdot \int dx_g^{true} A(x_g^{true}, x_g^{obs}) \cdot \frac{d\hat{\sigma}}{d\log\left(x_g^{true}\right)} \cdot f_{g/p}(x_g^{true}) \quad (2)$$

For both analyses NLO calculations fully differential in the four–momentum of the generated quarks are available [5,6]. The distributions of the $D^\star$ mesons are obtained by folding the distribution of the quark momenta with a Peterson fragmentation function.

Through the knowledge of $\hat{\sigma}$ and A, the measured cross sections $d\sigma/d\log(x_g^{obs})$ could be unfolded [7]. The resulting gluon densities shown in Figure 3 are in good agreement with with each other and with the results obtained from scaling violations of F_2 [8]. This agreement is a good confirmation of the universality of the gluon density function.

Table 1: Kinematic range of the measurements of $d\sigma/d\log x_g^{obs}$

Data	DIS	Photoproduction		
$\langle W\rangle$ [GeV]	120	88	185	223
y	$0.01\ldots0.7$	≈ 0.09	$0.29\ldots0.50$	$0.50\ldots0.62$
Q^2 [GeV^2]	$2\ldots100$	< 0.01	< 0.01	< 0.01
$p_\perp(D^\star)$ [GeV/c]	> 1.5	> 2.0	> 2.5	> 2.5
rapidity η pseudorapidity $\hat{\eta}$	-1.5 ... 1.5	0 ... 1.0	-1.5 ... 0.5	-1.5 ... 0.5
$\mathcal{L}$ [pb^{-1}]	2.33	10.2	10.7	10.7

Table 2: Parameters of the used NLO calculations.

	DIS	Photoproduction
NLO Calculation (massive scheme)	Smith & Harris [5]	Frixione, Mangano, Nason, Ridolfi [6]
μ_F^2	$Q^2+4m_c^2$	$4\cdot(p_\perp^2+m_c^2)$
μ_R^2	μ_F^2	$1/4\cdot\mu_F^2$
fragment. parameter ϵ_c	0.06 (0.02 ... 0.078)	0.035 ± 0.01
Λ_5	225 MeV	152 MeV
m_c	1.5 GeV/c^2	1.5 GeV/c^2

References

1. C. Adloff et al. (H1 Coll.), Contribution to IEC-HEP97, Jerusalem, 1997, Abstract 275;
   D. Müller, PhD Thesis, Universität Zürich (1998).
2. U. Bassler and G. Bernardi, Nucl. Inst. Meth. A362 (1995) 197.
3. H. Niggli, PhD Thesis, ETH–Zürich (1998).
4. R. van Wouldenberg et. al., Proc. of the Workshop *Physics at HERA*, 1991, vol. 2, p. 739.
5. B.W. Harris and J. Smith, DESY 97-111; Nucl.Phys. B 452(1995) 109.
6. R.K. Ellis and P. Nason, Nucl.Phys. B312 (1989) 551;
   P. Nason, S. Dawson, and R.K. Ellis, Nucl.Phys. B303 (1988) 607;
   J. Smith and W.L. Van Neerven, Nucl.Phys. B374 (1992) 36;
   S. Frixione et al., Phys.Lett. B348 (1995) 633;
   Nucl.Phys. B454 (1995) 3.
7. G. D'Agostini, Nucl. Inst. Meth. A362 (1995) 487.
8. V. Shekelian, DESY 97-248